Journal of Applied Physics ARTICLE scitation.org/journal/jap

Strain induced mobility enhancement in p-type silicon structures: Bulk and quantum well (quantum kinetic approach)

Cite as: J. Appl. Phys. **125**, 082515 (2019); doi: 10.1063/1.5045620
Submitted: 22 June 2018 · Accepted: 4 November 2018 ·
Published Online: 7 December 2018

K. L. Kovalenko, S. I. Kozlovskiy, and N. N. Sharan

AFFILIATIONS

Laboratory of Anisotropic Semiconductors, V. Lashkaryov Institute of Semiconductor Physics, National Academy of Sciences of Ukraine, 41, Prospect Nauki, 03028 Kyiv, Ukraine

ABSTRACT

Analytic expressions for low field mobility have been obtained in the high strained p-type silicon structures with three- and two-dimensional hole gases. Much attention is paid to study how confinement in one spatial dimension changes the strain mobility enhancement in comparison with bulk material. The mobility enhancement factor has been calculated when applying both the uniaxial and biaxial strains. Acoustic and optic phonons, charged impurities, and surface roughness have been accepted as a scattering system. Our theoretical consideration is based on the quantum kinetic equation and a special form of the non-equilibrium distribution function (shifted Fermi distribution). Results of the calculation are compared with known experimental data.

I. INTRODUCTION

Influence of elastic strain on transport in semiconductors has been a research topic for over half a century. Strain is considered to be the main tool to boost current and enhance mobility of advanced silicon-based field-effect transistors (FETs). The main advantage of the strain engineering technology is an opportunity to get higher mobility without dramatically changing the FET size and architecture.[1,2]

Various theoretical models were proposed to predict the strain mobility enhancement in FETs to make their design easier and design cycle shorter. The simplest approach for calculations of the strain-altered hole mobility in silicon is the Drude model,[3] $\mu = e\tau/m^*$ where μ is the carrier mobility, τ is the momentum relaxation time, and m^* is the conductivity effective mass. The strain changes the conductivity mass, and also the density of states in bands, which consequently affects the momentum relaxation time. The Drude model is sufficiently crude and can provide only a qualitative explanation for experimental observations.[4] A comparison with the experiment[3] shows that it may serve as a starting point to understand the basic transport properties in semiconductors.[4]

The more rigorous approach is solving the Boltzmann transport equation (BTE) in the relaxation time approximation (RTA).[5,6] For isotropic dispersion law, the RTA is sufficiently good. However, for semiconductors with complicated dispersion relations, some doubts have been raised regarding its validity. At high strains, the constant energy surfaces of heavy and light holes are transformed from practically isotropic corrugated spheres into ellipsoids with anisotropic effective masses.[7] In this case, applying the RTA is questionable.[8]

Theoretically, the simulation method capable of providing a "physically" exact solution of the BTE without invoking approximations is the Monte Carlo (MC) simulation.[9] In Refs. 10 and 11, the MC simulation was used for the theoretical study of the hole mobility response to high stress in bulk Si up to 3-4 GPa. The MC simulations of the transport phenomena are usually time-consuming and not always transparent. A major drawback of the MC simulation is its relatively high computational cost.[9] An analytical model to understand the underlying physics and determine optimal conditions for enhancement of the carrier mobility at strain is therefore required.

Calculations of the strain induced mobility enhancement factors in Ref. 11 are questionable as far as they have been carried out under the assumption that the relative changes in mobility are equal to the relative changes in resistivity at strain application. The proposed model ignored changes in density of holes that could exceed at high strains (up to 4 GPa) more than tenfold the hole density in the unstrained state.[12]

In this paper, we carry out a comparative study of the low field mobility in the high strained p-type silicon structures with three- and two-dimensional hole gases (3DHG and 2DHG, respectively). In particular, we are interested in how the reduced dimensionality in one spatial dimension influences the strain induced mobility enhancement as compared to bulk crystal and also the consequences this has for the hole transport in structures with 2DHG. For this purpose, we employ the method from first principles that is based on the quantum kinetic equation and a special form of the non-equilibrium distribution function (shifted Fermi distribution).

II. DISPERSION RELATIONS

A. Bulk material (3DHG)

For high strains, the majority of holes is located near the center of the Brillouin zone, and the constant energy surfaces of holes have forms of ellipsoids.[7] The directions of the principal axes of the ellipsoids (e.g., the Ox, Oy, and Oz axes) are determined by the strain tensor $\hat{e}$. The dispersion law of holes in the principal axes can be written as[12]

$$\varepsilon_v(\vec{k},\,\widehat{e})^{(D=3)} = \frac{\Delta_{SO}}{3} - aSp(\widehat{e}) - \Delta\varepsilon_v(\hat{e}) + \frac{\hbar^2}{2}\left[\frac{k_x^2}{m_{xx}^{(v)}} + \frac{k_y^2}{m_{yy}^{(v)}} + \frac{k_z^2}{m_{zz}^{(v)}}\right]. \tag{1}$$

$\varepsilon_v(\vec{k},\,\widehat{e})^{(D=3)}$ is energy of holes in the v-th sub-bund for 3DHG (D = 3), $\vec{k}$ is the wave vector, $\hbar$ is the reduced Plank constant, $\Delta\varepsilon_v(\hat{e})$ is amendment to energy of holes in the v-th sub-bund due to elastic strain, $\Delta_{SO} = 0.044$ eV is the spin-orbit split-off energy in the unstrained state, and $m_{xx(yy,zz)}^{(v)}$ are the effective masses of holes in the v-th sub-band. For cases considered here, expressions of effective masses are given in the Appendix. Sub-indexes $v = 1$ and $v = 2$ correspond to the bands of heavy and light holes in the unstrained state, respectively.

$\Delta\varepsilon_1(\hat{e}) = 2\,\cos(\pi/6+\chi)\gamma^{1/2}$, $\Delta\varepsilon_2(\hat{e}) = 2\gamma^{1/2}\sin\chi$, $\chi = \arcsin(\beta/\gamma^{3/2})/3$, $\beta = \Theta_{e3}/2 + \Delta_{SO}^3/27$, $\gamma = \Theta_{e2} + \Delta_{SO}^2/9$, $Sp(\hat{e}) = e_{xx} + e_{yy} + e_{zz}$, $\Theta_{e2} = b^2[(e_{xx}-e_{yy})^2 + (e_{yy}-e_{zz})^2 + (e_{zz}-e_{xx})^2]/2 + d^2(e_{xy}^2 + e_{xz}^2 + e_{zy}^2)$, $\Theta_{e3} = b^3[Sp(\hat{e}) - 3e_{zz}]^3 - 3\Theta_{e2}b[Sp(\hat{e}) - 3e_{zz}] + 9bd^2[(e_{yy}-e_{zz})e_{xz}^2 + (e_{xx}-e_{zz})e_{yz}^2] - 6\sqrt{3}d^3e_{xy}e_{zy}e_{xz}$.

Here a, b, and d are, respectively, dilatation, uniaxial, and shear deformation potentials.

B. Quantum well (2DHG)

An important system where quantum effects are observed is 2DHG in Si MOSFETs. At high strains, the difference in energy of the heavy and light hole sub-bands can reach more than 50 meV.[1,2] In this case, we may neglect by any coupling between the sub-bands.

The confining potential, we will approximate by the triangle quantum well that is widely used to describe energy bands in inversion layers.[13,14] The approximation allows the exact analytical solution of the Schrödinger equation in terms of Airy functions Ai(z):

$$\mathrm{Ai}(z) = \frac{1}{\pi}\int_0^\infty \cos\left(\frac{t^3}{3} + zt\right) dt. \tag{2}$$

The dispersion law for 2DHG $\varepsilon_{v,n}(\vec{k},\,\widehat{e})^{(D=2)}$ can be obtained from (1) by the following substitution:

$$\frac{\hbar^2 k_z^2}{2m_{zz}^{(v)}} \to \varepsilon_n^{(v)} = e(-a_n)E_{eff}L_E^{(v)}, \tag{3}$$

where z is the direction of quantum confinement, e is the absolute value of the electron charge, a_n is the n-th zero of the Airy function, n is the quantum number, $L_E^{(v)} = [\hbar^2/2m_{zz}^{(v)}eE_{eff}]^{1/3}$ is the characteristic length of quantum confinement, $m_{zz}^{(v)}$ is the effective mass of holes in the v-th sub-band in direction of the quantum confinement, and E_{eff} is the transverse effective field.[13–15] The zeros of the Airy function can be approximated by[13,14]

$$a_n \simeq -\left[\frac{3\pi}{2}\left(n - \frac{1}{4}\right)\right]^{2/3}, \quad n = 1, 2, \ldots \tag{4}$$

III. MOBILITY: QUANTUM KINETIC APPROACH

For *ab initio* calculation of low field mobility $\hat{\mu}$, we will use the quantum kinetic approach[16–18] that is based on the one-particle density matrix $\hat{\rho}$. The fundamental equation is[9,16–18]

$$i\hbar\frac{\partial\widehat{\rho}}{\partial t} = [\widehat{\rho}\widehat{H} - \widehat{H}\widehat{\rho}], \tag{5}$$

where $\widehat{H}$ is the Hamiltonian of the whole system.

Using the plane waves as basic wave-functions, quantum kinetic equation can be presented in the following form:[16–18]

$$\frac{e}{\hbar}\vec{E}\frac{\partial f_{\vec{k}}}{\partial\vec{k}} = \mathrm{St}f_{\vec{k}}. \tag{6}$$

$\vec{E}$ is the electric field, $\mathrm{St}f_{\vec{k}}$ is the collision integral, and $f_{\vec{k}}$ is the non-equilibrium distribution function. Here $f_{\vec{k}} = \langle a_{\vec{k}}^+ a_{\vec{k}}\rangle$, where $a_{\vec{k}}^+$ and $a_{\vec{k}}$ are, respectively, operators of creation and annihilation of the particle in the state $\vec{k}$; the value $a_{\vec{k}}^+ a_{\vec{k}} = \rho_{\vec{k}\vec{k}}$ is the diagonal component of the one-particle density matrix in $\vec{k}$-representation; the angular brackets designate statistical averaging of the shown operator together with non-equilibrium statistical operator of the whole system.

The collision integral can be presented as[16–18]

$$\mathrm{St}f_{\vec{k}} = -\frac{e^2}{(2\pi)^D\hbar^2}\int d^D\vec{q}\langle\phi^2\rangle_{\omega,\vec{q}}^{(D)} \times\left\{f_{\vec{k}} - f_{\vec{k}-\vec{q}} + [f_{\vec{k}}(1-f_{\vec{k}-\vec{q}}) + f_{\vec{k}-\vec{q}}(1-f_{\vec{k}})]\tanh\left(\frac{\hbar\omega}{2k_BT}\right)\right\}. \tag{7}$$

Here k_B is Boltzmann's constant, T is the temperature, and D is the dimensionality of the free carriers gas $D \in 1, 2, 3$. The

values D = 1, D = 2, and D = 3 correspond to the quantum wire, the quantum well, and bulk material, respectively. In expression (7), we have assumed that in the scattering process a hole makes a transition from some initial state $\vec{k}$ to the final state $\vec{k}' = \vec{k} - \vec{q}$; thus, $\hbar\vec{q}$ is the transferred momentum, $\varepsilon_{\vec{k}} - \varepsilon_{\vec{k}-\vec{q}} = \pm\hbar\omega_{\vec{q}}$ is the change in energy at collision, and $\langle\phi^2\rangle^{(D)}_{\omega,\vec{q}}$ is the spectral correlator of the scattering potential.

For the uniform scattering system[16–18]

$$\langle[\varphi(\omega,\vec{q}),\varphi(\omega_1,\vec{q}_1)]_+\rangle = (2\pi)^4\delta(\omega+\omega_1)\delta(\vec{q}+\vec{q}_1)\langle\varphi^2\rangle_{\omega,\vec{q}}, \quad (8)$$

where $\phi(\vec{q},\omega)$ is the Fourier-components of scattering potential and $[a,b]_+ = (1/2)(ab+ba)$. For the point impurities, the symbol of average in (7) and (8) concerns in the location of scattering centers in space; for phonons, it concerns in standard statistical distribution.

Approximating the non-equilibrium distribution function by the shifted Fermi distribution and performing the mathematical transforms given in Ref. 18, we obtain the expression for kinetic tensor $\hat{\lambda}$ which is the inverse to the mobility tensor $\hat{\lambda} = \hat{\mu}^{-1}$,[16–19]

$$\hat{\lambda}_v = -\frac{e\hbar}{(2\pi)^{2D}p_v^{(D)}k_BT}\int\frac{d\omega}{\sinh(\hbar\omega_{\vec{q}}/k_BT)}\int\vec{q}^2 < \varphi^2 >^{(D)}_{\omega,\vec{q}} d^D\vec{q} \times\int(f^0_{\vec{k}} - f^0_{\vec{k}-\vec{q}})\delta(\varepsilon^{(v)}_{\vec{k}} - \varepsilon^{(v)}_{\vec{k}-\vec{q}} \mp \hbar\omega_{\vec{q}})\Phi(\varepsilon_{\vec{k}} - \hbar\omega_{\vec{q}})d^D\vec{k}. \quad (9)$$

$p_v^{(D)}$ is the density of holes in the v-th sub-band and $f^0_{\vec{k}}$ is the equilibrium Fermi distribution function. The top sign in (9) applies for phonon emission and the bottom for phonon absorption. $\Phi(\varepsilon_{\vec{k}} - \hbar\omega_{\vec{q}})$ is the Heaviside step function that ensures a positive kinetic energy of holes for scattering with the emission of phonons (primarily for optic phonons).

For scattering by ionized impurities, expression (9) should be modified as

$$\omega_{\vec{q}} \to \omega,\ \delta(\varepsilon^{(v)}_{\vec{k}} - \varepsilon^{(v)}_{\vec{k}-\vec{q}} \mp \hbar\omega_{\vec{q}})\Phi(\varepsilon_{\vec{k}} - \hbar\omega_{\vec{q}}) \to \delta(\varepsilon^{(v)}_{\vec{k}} - \varepsilon^{(v)}_{\vec{k}-\vec{q}} - \hbar\omega). \quad (10)$$

The density of holes in the v-th sub-band is defined by the Fermi energy ε_F,

$$p_v^{(D)} = \frac{2}{(2\pi)^D}\int\frac{d^D\vec{k}}{\exp[(\varepsilon^{(v)}_{\vec{k}} - \varepsilon_F)/k_BT]+1}. \quad (11)$$

At mixed scattering, the kinetic tensor is a sum over scattering mechanisms

$$\lambda_v^{(\Sigma)} = (\lambda_v)_A + (\lambda_v)_O + (\lambda_v)_I + (\lambda_v)_{SR}, \quad (12)$$

where $(\hat{\lambda}_v)_A$, $(\hat{\lambda}_v)_O$, $(\hat{\lambda}_v)_I$, and $(\hat{\lambda}_v)_{SR}$ are the kinetic tensors for scattering of holes by acoustic, optic phonons, ionized impurities, and surface roughness, respectively.

IV. CORRELATORS OF SCATTERING POTENTIALS

In the frame of the proposed quantum kinetic approach, a scattering process of charged carriers is described by the correlators of scattering potential $\langle\varphi^2\rangle^{(D)}_{\omega,\vec{q}}$. A correlator can be associated with the per-unit-time probability of the charged carrier transition $W(\vec{k},\vec{k}')$ from the state $\vec{k}$ into the state $\vec{k}'$ by the following relation:[17]

$$W(\vec{k},\vec{k}') = \frac{e^2}{\hbar L^D}\left[1-\tanh\left(\frac{\varepsilon_{\vec{k}}-\varepsilon_{\vec{k}'}}{2k_BT}\right)\right]\int d\omega\,\delta(\varepsilon_{\vec{k}} - \varepsilon_{\vec{k}-\vec{q}} - \hbar\omega) \times\int\langle\varphi^2\rangle^{(D)}_{\omega,\vec{q}}\delta(\vec{k}-\vec{k}'-\vec{q})d^D\vec{q}, \quad (13)$$

where L is the linear dimension of the considered system.

A. Bulk material (3DHG)

Correlators of the random scattering potential for scattering by acoustic (deformation potential) and non-polar optic phonons have the following forms:[16,17,19]

$$\langle\varphi^2_A\rangle^{(D=3)}_{\omega,\vec{q},v} = \left(\frac{\Xi}{e}\right)^2\frac{\pi\hbar\omega}{2\rho s_L^2}\coth\left(\frac{\hbar\omega}{2k_BT}\right)[\delta(\omega - s_Lq) + \delta(\omega + s_Lq)], \quad (14)$$

$$\langle\varphi^2_O\rangle^{(D=3)}_{\omega,\vec{q}} = \left(\frac{D_0}{e}\right)^2\frac{\pi\hbar}{2\rho\omega_0}\coth\left(\frac{\hbar\omega_0}{2k_BT}\right)[\delta(\omega-\omega_0) + \delta(\omega+\omega_0)], \quad (15)$$

where ρ is the density of crystal, s_L is the longitudinal sound velocity, Ξ and D_0 are the acoustic and optical coupling constants, and $\hbar\omega_0$ is the energy of optic phonon.

B. Quantum well (2DHG)

Now we consider the scattering process in 2D systems. The spectral correlators for 2DHG and 3DHG differ by two things: momentum conservation applies in the plane $\vec{k} \to \vec{k}_\perp$ and $\vec{q} \to \vec{q}_\perp = \vec{k}_\perp - \vec{k}'_\perp$ (in our case the xy-plane) and the appearance of the form factor $F_{nm}(q_z)$ (z is the direction of the quantum confinement). The overlap integral defines the density profile of the charges in the quantum well.[13,14,20–22] For the quantum well with the potential walls that are impenetrable for charge carriers, the form factor has the following form:[21]

$$F_{nm}(q_z) = \int_0^\infty \exp(-iq_zz)\xi_n(z)\xi_m(z)dz, \quad (16)$$

where $\xi_n(z)$ and $\xi_m(z)$ are the envelope functions in the confined direction. In a triangular quantum well, the envelope functions with quantum numbers n and m are

$$\xi^{(v)}_{n(m)}(z) = \frac{1}{\sqrt{I_{n(m)}L_E^{(v)}}}\mathrm{Ai}\left[\frac{z}{L_E^{(v)}} + a_{n(m)}\right], \quad I_{n(m)} = \int_0^\infty \mathrm{Ai}(y + a_{n(m)})^2dy. \quad (17)$$

Expressions for the 2DHG spectral correlators for scattering by

acoustic $\langle\varphi_A^2\rangle_{\omega,\vec{q}_\perp}^{(D=2)}$ and optic $\langle\varphi_O^2\rangle_{\omega,\vec{q}_\perp}^{(D=2)}$ phonons can be obtained from 3DHG correlators by integration:[16,17]

$$\langle\varphi^2\rangle_{\omega,\vec{q}_\perp}^{(D=2)} = \frac{1}{2\pi}\int_{-\infty}^{\infty}\langle\varphi^2\rangle_{\omega,\vec{q}}^{(D=3)}|F_{nm}(q_z)|^2 dq_z. \quad (18)$$

After integration, we obtain

$$\langle\varphi_A^2\rangle_{v,\omega,q_\perp}^{(D=2)} = \delta_{nm}\left(\frac{\Xi}{e}\right)^2\frac{\pi\hbar\omega^2}{2\rho s_L^2}\coth\left(\frac{\hbar|\omega|}{2k_BT}\right)\frac{\Phi(\omega^2-q_\perp^2 s_L^2)}{\sqrt{\omega^2-q_\perp^2 s_L^2}}, \quad (19)$$

where δ_{nm} is the Kronecker delta.

Finally, in elastic scattering approximation $\hbar|\omega| \ll k_BT$ expression, (19) is simplified to

$$\langle\varphi_A^2\rangle_{\omega,\vec{q}}^{(D=2)} = \delta_{nm}\left(\frac{\Xi}{e}\right)^2\frac{k_BT}{\rho s_L^3}\delta(\omega). \quad (20)$$

Similar integration gives a correlator for scattering by optic phonons

$$\langle\varphi_O^2\rangle_{v,\omega,\vec{q}_\perp}^{(D=2)} = \left(\frac{D_0}{e}\right)^2\frac{A_{nm}^{(O)}\pi\hbar\coth(\hbar\omega_0/2k_BT)}{2\rho\omega_0 L_E^{(v)}}[\delta(\omega-\omega_0)+\delta(\omega+\omega_0)], \quad (21)$$

where

$$A_{nm}^{(O)} = \frac{1}{2\pi I_n I_m}\int_{-\infty}^{\infty}\left|\int_0^{\infty}\exp(-ixz)Ai(z+a_n)Ai(z+a_m)dz\right|^2 dx. \quad (22)$$

For scattering by ionized impurities, the spectral correlator is given by[23]

$$\langle\varphi_I^2\rangle_{\omega,q_\perp}^{(D=2)} = \frac{(2\pi)^3 e^2 N_I^{(D=2)} A_{n,m}^{(I)}(q_\perp)^2}{\varepsilon_L^2 q_\perp^2}\delta(\omega), \quad (23)$$

where $N_I^{(D=2)}$ is the areal density of scattering centers. The overlap integral $A_{v,n,m}^{(I)}(q_\perp)$ is defined as

$$A_{v,n,m}^{(I)}(q_\perp) = \frac{1}{I_n I_m}\int_0^{\infty}\exp(-|\vec{q}_\perp|L_E^{(v)}z)Ai(z+a_n)Ai(z+a_m)dz. \quad (24)$$

Fluctuation of the quantized energy of charge carriers in the quantum well due to fluctuation of its width causes additional scattering named surface roughness scattering.[20,22–26] If the interface roughness is assumed to be characterized by the lateral size Λ and height Δ of Gaussian fluctuations of the interface the correlator is given[23]

$$\langle\varphi_{SR}^2\rangle_{\omega,q_\perp}^{(D=2)} = 2\pi^2\Delta^2\Lambda^2\exp(-q_\perp^2\Lambda^2/4)E_{eff}^2\delta(\omega). \quad (25)$$

V. MOBILITY

Thus, calculations of the mobility have been performed in the following assumptions:

- The model non-equilibrium distribution function has a form the shifted Fermi distribution.
- The drift velocity of holes is proportional to electric field $\vec{E}$ and is significantly less than the thermal velocity.
- Majority of holes is located near of the center of the Brillouin zone (the high strain approximation[7]). In this case, the mobility tensor has a diagonal form with principal axes that are set by the strain tensor.
- The confining potential of the 2DHG is approximated by the triangular quantum well.

A. Bulk material (3DHG)

Integration (9) with dispersion law (1) and correlator (15) gives the following expressions for components of the mobility tensor for scattering by optic phonons $\mu_O^{(v)}$ in the v-th sub-band

$$\mu_{O\,xx(yy,zz)}^{(v)} = \delta_{ij}\frac{3(2\pi)^{3/2}(k_BT)^{1/2}\hbar^2\rho x_0}{2(D_o/e)^2 e m_{xx(yy,zz)}^{(v)3/2}}\frac{\sinh(x_0/2)^2 F_{1/2}(\eta_v^{(D=3)})}{\sqrt{m_{yy(xx,zz)}^{(v)}m_{zz(yy,xx)}^{(v)}}} \times\left\{\int_0^{\infty}dx[f^0(\eta_v^{(D=3)},x)-f^0(\eta_v^{(D=3)},x+x_0)](2x+x_0)\sqrt{x(x+x_0)}\right\}^{-1}. \quad (26)$$

Here $\eta_v^{(D=3)} = [\varepsilon_F - \Delta\varepsilon_v(\hat{e})]/k_BT$ and $f^0(\eta,x)$ is Fermi-Dirac equilibrium distribution function, $F_r(\eta)$ are Fermi integrals

$$F_r(\eta) = \frac{1}{\Gamma(r+1)}\int_0^{\infty}\frac{x^r dx}{\exp(x-\eta)+1}. \quad (27)$$

Expressions for mobility of 3DHG for scattering by acoustic phonons and ionized impurities were obtained in Ref. 23.

B. Quantum well (2DHG)

With dispersion relations integration (9) give the following expressions for components of the kinetic tensor for scattering holes by acoustic (A) and optic (O) phonons, respectively,

$$\mu_{v,n,m,xx(yy)}^{(A)} = \delta_{ij}\delta_{nm}\frac{4}{\pi}\frac{\rho s^3\hbar^4}{(\Xi/e)^2 e(k_BT)^2 m_{xx(yy)}^{(v)}m_{yy(xx)}^{(v)}{}^{1/2}}, \quad i,j\in x,y \quad (28)$$

$$\mu_{v,n,m}^{(O)} = \delta_{ij}\frac{16}{3}\frac{\hbar\rho x_0\sinh(x_0/2)^2 k_BT L_E^{(v)}F_0(\eta_{v,n}^{(D=2)})}{(D_0/e)^2 e m_{xx(yy)}^{(v)}\sqrt{m_{xx}^{(v)}m_{yy}^{(v)}}A_{nm}^{(O)}} \times\left\{\int_0^{\infty}(2x+x_0)[f_0(x,\eta_{v,n}^{(D=2)})-f_0(x+x_0,\eta_{v,n}^{(D=2)})]dx\right\}^{-1}. \quad (29)$$

Here

$$A_{nm}^{(O)} = \frac{1}{2\pi I_n I_m}\int_{-\infty}^{\infty}\left|\int_0^{\infty}\exp(-ixz)Ai(z+a_n)Ai(z+a_m)dz\right|^2 dx, \quad (30)$$

$\eta_{v,n}^{(D=2)} = \eta_v^{(D=3)} - (-a_n)eE_{eff}L_E^{(v)}$, $f_0(x,\eta) = [\exp(x-\eta)+1]^{-1}$ is the Fermi distribution function.

For scattering by ionized impurities, the components of the kinetic tensor are

$$\begin{cases}\lambda_{v,n,xx}^{(I)}\\ \lambda_{v,n.yy}^{(I)}\end{cases} = \delta_{ij}\delta_{nm}\frac{e^3N^{(D=2)}m_{xx(yy)}^{(v)\,3/2}m_{yy(xx)}^{(v)\,1/2}}{k_BT\varepsilon_L^2\hbar F_0(\eta_v^{(D=2)})}\int_0^{2\pi}\begin{matrix}\cos(\varphi)^2\\ \sin(\varphi)^2\end{matrix}d\varphi$$
$$\times\int_0^1 dz\int_0^\infty dx\left(-\frac{\partial f_0(x,\eta_{v,n}^{(D=2)})}{\partial x}\right)\frac{A_{v,n,m}^{(I)}(z,x,\varphi)^2}{(m_{xx}^{(v)}\cos(\varphi)^2+m_{yy}^{(v)}\sin(\varphi)^2)\sqrt{1-z^2}}. \quad (31)$$

Here

$$A_{v,n,m}^{(I)}(z,x,\varphi) = \frac{1}{I_nI_m}\int_0^\infty \exp\left[-zyL_E^{(v)}\sqrt{\beta_v(x,\varphi)}\right]Ai(y+a_n)Ai(y+a_m)dy, \quad (32)$$

$$\beta_v(x,\varphi) = 8k_BTx(m_{xx}^{(v)}\cos(\varphi)^2+m_{yy}^{(v)}\sin(\varphi)^2)/\hbar^2.$$

In the limit of small $|\vec{q}|$, $A_{v,n,m}^{(I)}(z,x,\varphi)\approx\delta_{nm}$ and expression (32) simplifies

$$\lambda_{v,xx(yy)}^{(I)} = \frac{e^3N^{(D=2)}m_{xx}^{(v)}\sqrt{m_{xx}^{(v)}m_{yy(xx)}^{(v)}}}{k_BT\varepsilon_L^2\hbar\left[\sqrt{m_{xx}^{(v)}}+\sqrt{m_{yy}^{(v)}}\right]}\frac{F_{-1}(\eta_{v,n}^{(D=2)})}{F_0(\eta_{v,n}^{(D=2)})}, \quad (33)$$

where $F_{-1}(\eta) = [\exp(-\eta)+1]^{-1}$ and $F_0(\eta) = \ln[1+\exp(\eta)]$.

Below the areal density of the charged scattering centers $N_{I,v}^{(D=2)}$, we associate with volume concentration of scattering centers $N_I^{(D=3)}$ by the following relation $N_{I,v}^{(D=2)} = N_I^{(D=3)}L_E^{(v)}$.

For scattering by surface roughness integration (9) with correlator (25) gives

$$\mu_{v,n,m,xx(yy)}^{(SR)} = \delta_{ij}\delta_{nm}\frac{e\hbar^3F_0(\eta_{v,n}^{(D=2)})}{2e^2E_{eff}^2\Delta^2\Lambda^2m_{xx(yy)}^{(v)\,3/2}m_{yy(xx)}^{(v)\,1/2}}$$
$$\times\left\{\int_0^1\frac{z^2\exp(-\Theta_vz^2x)}{\sqrt{1-z^2}}dz\int_0^\infty\left[-\frac{\partial f_0[x,\eta_{v,n}^{(D=2)}]}{\partial x}\right]xdx\right\}^{-1}, \quad (34)$$

where $\Theta_v = 2m_vk_BT\Lambda^2/\hbar^2$. On practice $\Theta_v \ll 1$ and expression (34) can be simplified to

$$\mu_{v,xx(yy)}^{(SR)} = \delta_{ij}\frac{2}{\pi}\frac{\hbar^3}{e(\Delta\Lambda E_{eff})^2m_{xx(yy)}^{(v)\,3/2}m_{yy(xx)}^{(v)\,1/2}}. \quad (35)$$

Expressions for components of the mobility tensor we obtain by summation

$$\mu_{ij} = \delta_{ij}\frac{\sum_v\sum_n\left[p_{v,n}/\sum_m\lambda_{v,n,m}^{(\Sigma)}\right]}{\sum_v\sum_n p_{v,n}}, \quad i,j\in x,y. \quad (36)$$

The density of holes $p_{v,n}$ we obtain by integration (11) with dispersion law (3)

$$p_{v,n}^{(D=2)} = \frac{k_BT\sqrt{m_{xx}^{(v)}m_{yy}^{(v)}}}{\pi\hbar^2}F_0(\eta_{v,n}^{(D=2)}). \quad (37)$$

VI. DISCUSSION

In this section, we present calculations of the stress mobility enhancement factor in 3DHG and 2DHG systems and their comparison with known experimental data.

In calculations, we assumed the following numerical data:[27] the valence band constants (in units of $\hbar^2/2m_0$, where m_0 is free electron mass): $A = -4.28$, $B = -0.68$, $D = -5.04$, $C^2 = D^2 - 3B^2$, $\varepsilon_L = 11.7$, $\hbar\omega_0 = 61.2$ meV, $s_L = 8.4\times10^3$ m/sec, $\rho = 2.33\times10^3$ kg/m^3 deformation potentials (eV): $a = -10$, $b = -2.14$, $d = -5$, and values of elastic compliance constants (Pa^{-1}): $s_{11} = 0.768\times10^{-11}$, $s_{12} = -0.214\times10^{-11}$, and $s_{44} = 1.26\times10^{-11}$. The coupling constants for scattering by acoustic and optic phonons were employed $\Xi = 10$ eV and $D_0 = 3\times10^9$ eV/cm, respectively.[19] The values of parameters at the surface roughness scattering were accepted as $\Delta = 1.03$ nm and $\Lambda = 0.27$ nm.[24]

A. Biaxial strain

Experimental[28–35] and calculated dependences of mobility enhancement factors for 3DHG as a function of biaxial strain are shown in Figs. 1 and 2. Calculated dependences on base quantum kinetic equation are shown by solid lines. In calculations, the hole density was adopted as 10^{18} cm^{-3}. The dashed line in Fig. 1 shows theoretical dependence from Ref. 28

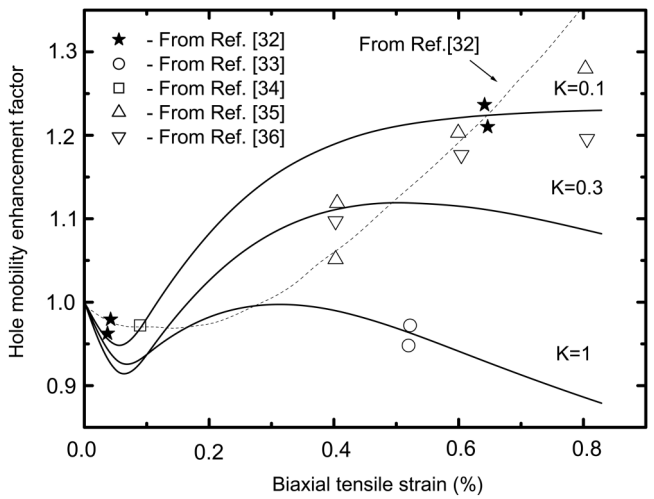

FIG. 1. Experimental[28–32] (figures) and calculated (lines) dependences of mobility enhancement factors are shown as a function of biaxial strain. The dashed line demonstrates results of calculation in relaxation time approximation from Ref. 28. Solid lines represent results of our calculations at different values of the biaxial stress non-uniformity factor *K*.

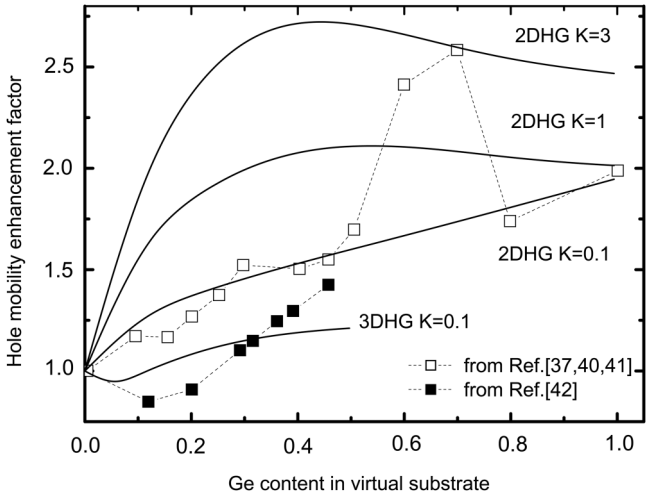

FIG. 2. Experimental (figures)[32–35] and calculated (solid lines) hole mobility enhancement in Si p-MOSFETs with 2D and 3D hole gases under wafer-based biaxial strain. Solid lines represent the results of calculations at different values of the biaxial stress non-uniformity factor *K*.

obtained in relaxation time approximation. This dependence is in qualitative agreement with the experiment but does not explain a wide scattering of the experimental data. We have obtained a better agreement with all experimental data in the assumption of the non-uniform biaxial stress where the magnitudes of stress components X_1 and X_2 are related by the non-uniformity factor $K = X_2/X_1$. The value $K = 1$ corresponds to the uniform biaxial stress. As displayed in Fig. 1 the highest mobility enhancement factor is obtained for $K = 0.1$, when the stress component in the [001] crystallographic direction is tenfold less than the component in the [110] direction. In this case, the biaxial strain is transformed into the practically uniaxial strain along the [110] crystallographic direction. Direct measurements of the stress components in strained SiGe nanostructures by liquid-immersion Raman spectroscopy[36] support our assumption about possible non-uniformity of biaxial stress in these nanostructures. The stress state could change from a uniform biaxial state to a practically uniaxial state.

The comparison of calculated and experimental[37–40] data in Si p-MOSFETs with 2DHG is represented in Fig. 3. MOSFETs with 2DHG exhibit a significant relative growth of mobility with the factor K in contrast to similar dependences in Fig. 1 for MOSFETs with 3DHG. We cannot explain the experimental dependence in Fig. 2 from Ref. 35 by transport of 2DHG. This dependence is in better agreement with our calculation results for 3DHG at $K = 0.1$.

B. Uniaxial strain

Figure 3 demonstrates experimental[37–40] and calculated dependences of the mobility enhancement factors in structures with 2D and 3D hole gases on strain along the [100] and [110] crystallographic directions. At strain along the [100] crystallographic directions, the calculated stress dependence of the mobility enhancement factor are in agreement with the experiment.

As it is shown in Fig. 4, the mobility enhancement factor depends on values of the transverse effective field E_{eff} and concentration of the ionized impurities. The enhancement factor reaches the maximum for moderate values of $E_{eff} \leq 1$ MV/m and at enough high concentrations of the ionized

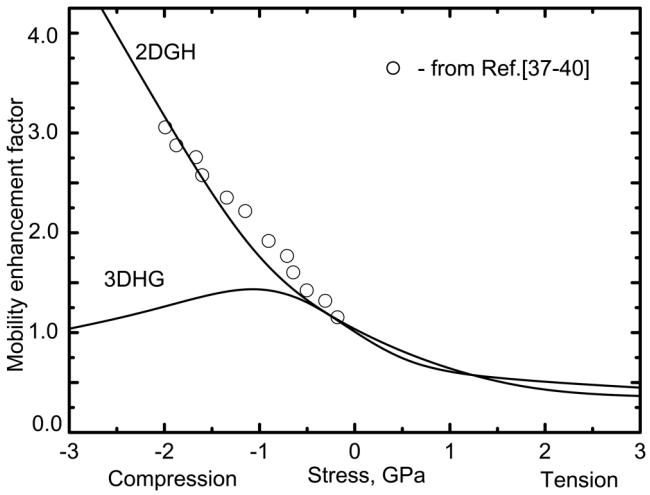

FIG. 3. Calculated (lines) and experimental (symbols) data stress-enhanced mobility are shown as function stress along the [100] crystallographic direction for $E_{eff} = 1$ MV/m and $N_I = 4 \times 10^{19}$ cm^{-3}.

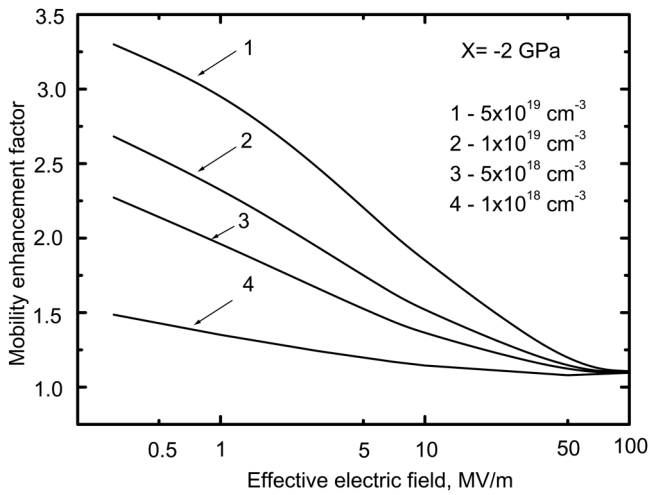

FIG. 4. Calculated dependences of the mobility enhancement factor on transverse effective field for different concentration of ionized impurities at uniaxial stress $X = -2$ GPa along the [100] crystallographic direction.

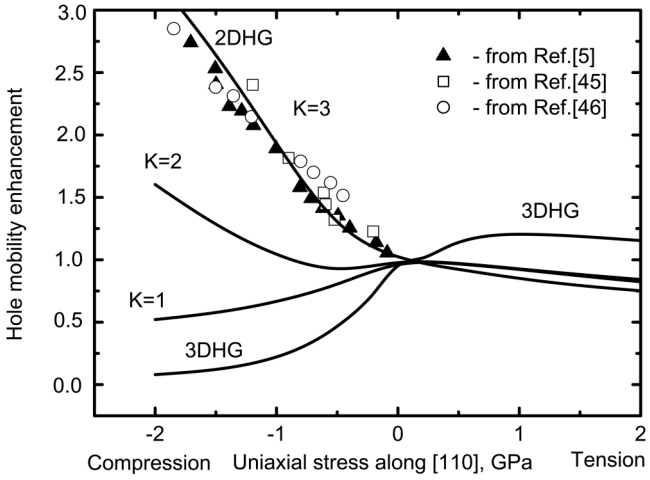

FIG. 5. Experimental (symbols) and calculated (lines) dependences of the hole mobility enhancement factor in p-Si structures with 3DHG and 2DHG under uniaxial stress along the [110] crystallographic direction. Calculated dependences for 2DHG are shown for different values of the strain concentration factor *K*.

impurities $N > 5 \times 10^{18}$ cm^{-3}. In Fig. 4, we see the strong dependence of the mobility enhancement factor for 2DHG on concentration of the ionized impurities. Our calculations show that this dependence is noticeably smaller for 3DHG. A large uniaxial strain effect on the mobility enhancement factor of 2DHG we associate with features of the impurity scattering of holes in two dimensions.

For uniaxial stress along the [110] crystallographic direction, our calculation predicts the decrease in the mobility enhancement factor for compressive strains (see Fig. 5 curve for $K = 1$) in contradiction to experimental data.[41]

Better agreement can be obtained in the assumption of the stress raisers effect. In practice, the stress patterns in p-MOSFETs are seldom as simple as a perfectly uniaxial or a perfectly biaxial.[41] In calculation, we have introduced the stress concentration factor (or stress raiser) K that describes an increase of the strain tensor diagonal components in plane of the channel $e_{xx} = e_{yy} = K(s_{11} + s_{12})X/2$. The value $K = 1$ corresponds to the perfectly uniaxial strain (see the Appendix). Mobility enhancement factor for different values of the stress concentration factor are shown in Fig. 5. The stress concentration of 2.8 is expected for agreement with the experiment.

The additional sources of the flat stress can be all intentional and unintentional stress sources as well as the stress evolution during the entire process flow such as thermal mismatch due to temperature ramps, lattice mismatch from epitaxial grain growth, intrinsic stress due to material bonding, force rebalance after etching, deposition, thinning, bumping, stacking, and packaging.[42,43]

VII. CONCLUSION

Analytical expressions for the low field mobility in the high strained p-type silicon structures with 3DHG and 2DHG have been obtained in the frame of quantum kinetic approach. We explain a wide range scattering of experimental data for the stress mobility enhancement factor at biaxial strain by its heterogeneity. At uniaxial strains, the stress mobility enhancement factor for 2DHG is significantly higher than for 3DHG. Calculated mobility enhancement factors for 2DHG at uniaxial compression along the [110] crystallographic direction are significantly less than was observed in the experiment. We associate the high experimental values of the stress-enhanced mobility under uniaxial compression along the [110] crystallographic direction with the concentration of the flat stresses that arises in the fabrication process of the field-effect transistors.

ACKNOWLEDGMENTS

The authors thank Dr. Alex V. Romanov for valuable help.

APPENDIX: COMPONENTS OF STRAIN AND EFFECTIVE MASS TENSORS

Below, we adduce expressions for the non-vanished components of the strain tensor for both uniaxial and biaxial strains.

At uniaxial stresses along the [100] and [110] crystallographic directions, the strain components are expressed, respectively, $e_{xx} = e_{yy} = s_{11}X$, $e_{zz} = s_{12}X$ and $e_{xx} = e_{yy} = (s_{11} + s_{12})X/2$, $e_{zz} = s_{12}X$, and $e_{xy} = s_{44}X/4$.

For non-uniform biaxial stress, the strain components are[44]

$$e_{xx} = e_{yy} = (s_{11} + s_{12})X_1/2 + s_{12}X_2,\ e_{zz} = s_{12}X_1 + s_{11}X_2,$$
$$e_{xy} = -s_{44}X_1/4.$$

Here, the stress components X_1 and X_2 directed along the [110] and [001] crystallographic directions, respectively.

At biaxial and uniaxial strains along the [110] direction, the effective masses in expression could be represented in the following forms:[7,11]

$$m^{(v)}_{xx(yy)} = \frac{\hbar^2}{2}(-A - \Theta^{(v)}_{2e}[Bb(e_{xx} - e_{zz}) \mp Dde_{xy} - 3\Theta^{(v)}_{3e}] \times \{B[b^2(e_{xx} - e_{zz})^2 - d^2e^2_{xy}] \pm 2Db(e_{xx} - e_{zz})e_{xy}d\})^{-1},$$

$$m^{(v)}_{zz} = \frac{\hbar^2}{2}\{-A + 2\Theta^{(v)}_{2e}Bb(e_{xx} - e_{zz}) + 6B\Theta^{(v)}_{3e}[b^2(e_{xx} - e_{zz})^2 - d^2e^2_{xy}]\}^{-1}.$$

At uniaxial strain along the [100] direction, the effective masses are

$$m^{(v)}_{xx(yy)} = \frac{\hbar^2}{2}(-\mathrm{A} \mp 2\Theta^{(v)}_{2e}Bb(e_{xx}-e_{yy}) + \Theta^{(v)}_{3e}Bb^2\{(Sp(\hat{e})-3e_{zz})[6e_{yy(xx)}-3e_{xx(yy)}-Sp(\hat{e})]+(Sp(\hat{e})-3e_{xx})(Sp(\hat{e})-3e_{yy})\})^{-1},$$

$$m^{(v)}_{zz} = \frac{\hbar^2}{2}(-\mathrm{A}+\Theta^{(v)}_{2e}Bb(e_{xx}-e_{yy})+\Theta^{(v)}_{3e}Bb^2 \times \{(Sp(\hat{e})-3e_{zz})[2Sp(\hat{e})-3(e_{xx}+e_{yy})]-2(Sp(\hat{e})-3e_{xx})(Sp(\hat{e})-3e_{yy})\})^{-1}.$$

Here

$$Q^{(1)}_{2e} = \gamma^{-1/2}\cos\left(\frac{\pi}{6}+\chi\right)+\frac{\beta\sin(\pi/6+\chi)}{(\gamma^4-\beta^2\gamma)^{1/2}},\ Q^{(2)}_{2e}=\gamma^{-1/2}\sin(\chi)-\frac{\beta\cos(\chi)}{(\gamma^4-\beta^2\gamma)^{1/2}},$$

$$Q^{(1)}_{3e} = -\frac{1}{3}\left(\gamma^2-\frac{\beta^2}{\gamma}\right)^{-1/2}\sin\left(\frac{\pi}{6}+\chi\right),\ Q^{(2)}_{3e}=\frac{1}{3}\left(\gamma^2-\frac{\beta^2}{\gamma}\right)^{-1/2}\cos(\chi).$$

REFERENCES

[1]V. Sverdlov, *Strain-Induced Effects in Advanced MOSFETs* (Springer-Verlag, Wien, 2011).
[2]D. Esseni, P. Palestri, and L. Selmi, *Nanoscale MOS Transistors. Semi-Classical Transport and Applications* (Cambridge University Press, 2011).
[3]Y. Sun, S. E. Thompson, and T. Nishida, J. Appl. Phys. **101**, 104503 (2007).
[4]Y. Sun, S. E. Thompson, and T. Nishida, *Strain Effect in Semiconductors. Theory and Device Applications* (Springer, New York, 2010).
[5]S. E. Thompson, G. Sun, Y. S. Choi, and T. Nishida, IEEE Trans. Electron Devices **53**, 1010 (2006).
[6]G. Sun, Y. Sun, T. Nishida, and S. E. Thompson, J. Appl. Phys. **102**, 084501 (2008).
[7]G. L. Bir and G. E. Pikus, *Symmetry and Strain Induced Effects in Semiconductors* (Wiley, New York, 1974).
[8]M. Lundstrom, *Fundamentals of Carrier Transport* (Cambridge University Press, 2000).
[9]M. V. Fischetti and W. G. Vandenberghe, *Advanced Physics of Electron Transport in Semiconductors and Nanostructures* (Springer, 2016).
[10]F. M. Bufler, A. Erlebach, and M. Oulmane, IEEE Electron Device Lett. **30**, 996 (2009).
[11]X.-F. Fan, L. F. Register, B. Winstead, M. C. Foisy, W. Chen, X. Zheng, B. Ghosh, and S. K. Banerjee, IEEE Trans. Electron Devices **54**(2), 291 (2007).
[12]S. I. Kozlovskiy and N. N. Sharan, J. Comput. Electron. **10**, 258 (2011).
[13]T. Ando, A. B. Fowler, and F. Stern, Rev. Mod. Phys. **54**(2), 437 (1982).
[14]D. K. Ferry, S. M. Goodnick, and J. Bird, *Transport in Nanostructures*, 2nd ed. (Cambridge University Press, Cambridge, 2009).
[15]S. M. Sze and K. K. Ng, *Physics of Semiconductor Devices*, 3rd ed. (John Wiley & Sons, Inc., 2007).
[16]I. I. Boiko, *Kinetics of Electron Gas Interacting with Fluctuating Potential* (Naukova Dumka, Kiev, 1993).
[17]I. I. Boiko, *Transport of Carriers in Semiconductors* (V. Lashkaryov Institute of Semiconductor Physics, NAS of Ukraine, Kyiv, 2009).
[18]I. I. Boiko and S. I. Kozlovskiy, Sens. Actuators A **147**, 17 (2008).
[19]S. I. Kozlovskiy and N. N. Sharan, J. Comput. Electron. **14**, 788 (2015).
[20]I. Knezevic, E. B. Ramayya, D. Vasileska, and S. M. Goodnick, J. Comput. Theor. Nanosci. **6**, 1725 (2009).
[21]M. A. Stroscio and M. Dutta, *Phonons in Nanostructures* (Cambridge University Press, 2001).
[22]Y. Ando and A. Cappy, J. Appl. Phys. **74**, 3983 (1993).
[23]K. L. Kovalenko, S. I. Kozlovskiy, and N. N. Sharan, J. Comput. Electron. **17**, 926 (2018).
[24]A. Pirovano, A. L. Lacaita, G. Zandler, and R. Oberhuber, IEEE Trans. Electron Devices **47**, 718 (2000).
[25]I. Watanabe, K. Kanzaki, T. Kitada, M. Yamamoto, S. Shimomura, and S. Hiyamizu, J. Cryst. Growth **251**, 90 (2003).
[26]S. Jin, M. V. Fischetti, and T.-W. Tang, IEEE Trans. Electron Devices **54**, 2191 (2007).
[27]P. Y. Yu and M. Cardona, *Fundamentals of Semiconductors. Physics and Material Properties*, 4th ed. (Springer, Heidelberg, 2010).
[28]M. H. Liao, S. T. Chang, M. H. Lee, S. Maikap, and C. W. Liua, J. Appl. Phys. **98**, 066104 (2005).
[29]K. Rim, J. Chu, H. Chen, K. A. Jenkins, T. Kanarsky, K. Lee, A. Mocuta, H. Zhu, R. Roy, J. Newbury, J. Ott, K. Petrarca, P. Mooney, D. Lacey, S. Koester, K. Chan, D. Boyd, M. Ieong, and H.-S. Wong, in *I Proceedings of the Symposium on VLSI Technology, Honolulu, HI* (IEEE, 2002), p. 98.
[30]K. Uchida, R. Zednik, C.-H. Lu, H. Jagannathan, J. McVittie, P. C. McIntyre, and Y. Nishi, in *Technical Digest—International Electron Devices Meeting* (IEEE, 2004), p. 229.
[31]S. Takagi, T. Mizuno, T. Tezuka, N. Sugiyama, and T. Numata, in *Technical Digest—International Electron Devices Meeting* (IEEE, 2003).
[32]C. W. Leitz, M. T. Currie, M. L. Lee, Z.-Y. Cheng, D. A. Antoniadis, and E. A. Fitzgeral, J. Appl. Phys. **92**, 3745 (2002).
[33]M. L. Lee, E. A. Fitzgerald, M. T. Bulsara, M. T. Currie, and A. Lochtefeld, J. Appl. Phys. **97**, 011101 (2005).
[34]M. T. Currie, C. W. Leitz, T. A. Langdo, G. Taraschi, E. A. Fitzgerald, and D. A. Antoniadis, J. Vac. Sci. Technol. B **19**, 2268 (2001).
[35]K. Rim, K. Chan, L. Shi, D. Boyd, J. Ott, N. Klymko, F. Cardone, L. Tai, S. Koester, and M. Cobb, in *Technical Digest—International Electron Devices Meeting, Washington, DC* (IEEE, 2003), p. 49.
[36]D. Kosemura, M. Tomita, K. Usuda, T. Tezuka, and A. Ogura, Jpn. J. Appl. Phys. **52**(45), 04CA05 (2013).
[37]F. Conzatti, M. De Michielis, D. Esseni, and P. Palestri, Solid-State Electron. **53**, 706 (2009).
[38]S. E. Thompson, M. Armstrong, C. Auth, S. Cea, R. Chau, G. Glass, T. Hoffman, J. Klaus, Z. Ma, B. Mcintyre, A. Murthy, B. Obradovic, L. Shifren, S. Sivakumar, S. Tyagi, T. Ghani, K. Mistry, M. Bohr, and Y. El-Mansy, IEEE Electron Device Lett. **25**, 191 (2004).
[39]E. Wang, P. Matagne, L. Shifren, B. Obradovic, R. Kotlyar, S. Cea, J. He, Z. Ma, R. Nagisetty, S. Tyagi, M. Stettler, and M. D. Giles, in *Electron Device Meeting IEDM Technical Digest* (IEEE, 2004), 147.

[40]L. Smith, V. Moroz, G. Eneman, P. Verheyen, F. Nouri, L. Washington, M. Jurczak, O. Penzin, D. Pramanik, and K. DeMeyer, IEEE Electron Device Lett. **26**, 652 (2005).
[41]L. Washington, F. Nouri, S. Thirupapuliyur, G. Eneman, P. Verheyen, V. Moroz, L. Smith, X. Xu, M. Kawaguchi, T. Huang, K. Ahmed, M. Balseanu, L.-Q. Xia, M. Shen, Y. Kim, R. Rooyackers, K. De Meyer, and R. Schreutelkamp, IEEE Electron Device Lett. **27**, 511 (2006).
[42]V. Moroz, N. Strecker, X. Xu, L. Smith, and I. Bork, Mat. Sci. Semicond. Proc. **6**, 27 (2003).
[43]X. Xu and V. Moroz, Mater. Res. Soc. Symp. Proc. **863**, B8.25 (2005).
[44]J. Kim, Ph.D. dissertation, Department of Electrical and Computer Engineering, University of Massachusetts, Amherst, USA, 2011. Open Access Dissertations. Paper 342, see http://scholarworks.umass.edu/open_access_dissertations/342.